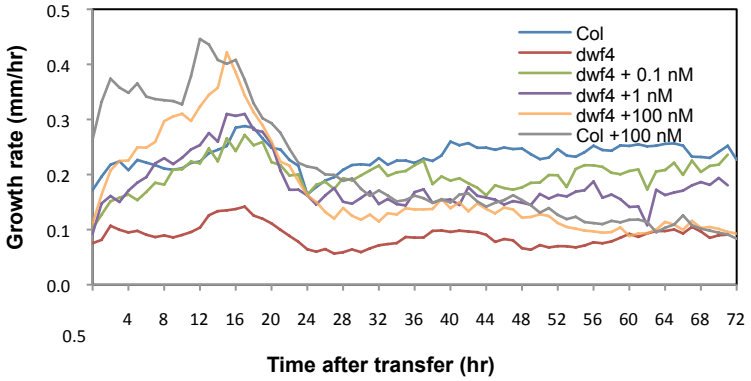

Figure S1. Brassinosteroid regulates dynamics of root growth.
Quantification of growth rates of wild-type and *dwf4* roots transferred to media with various concentrations of BL or mock. See also Figure 1.

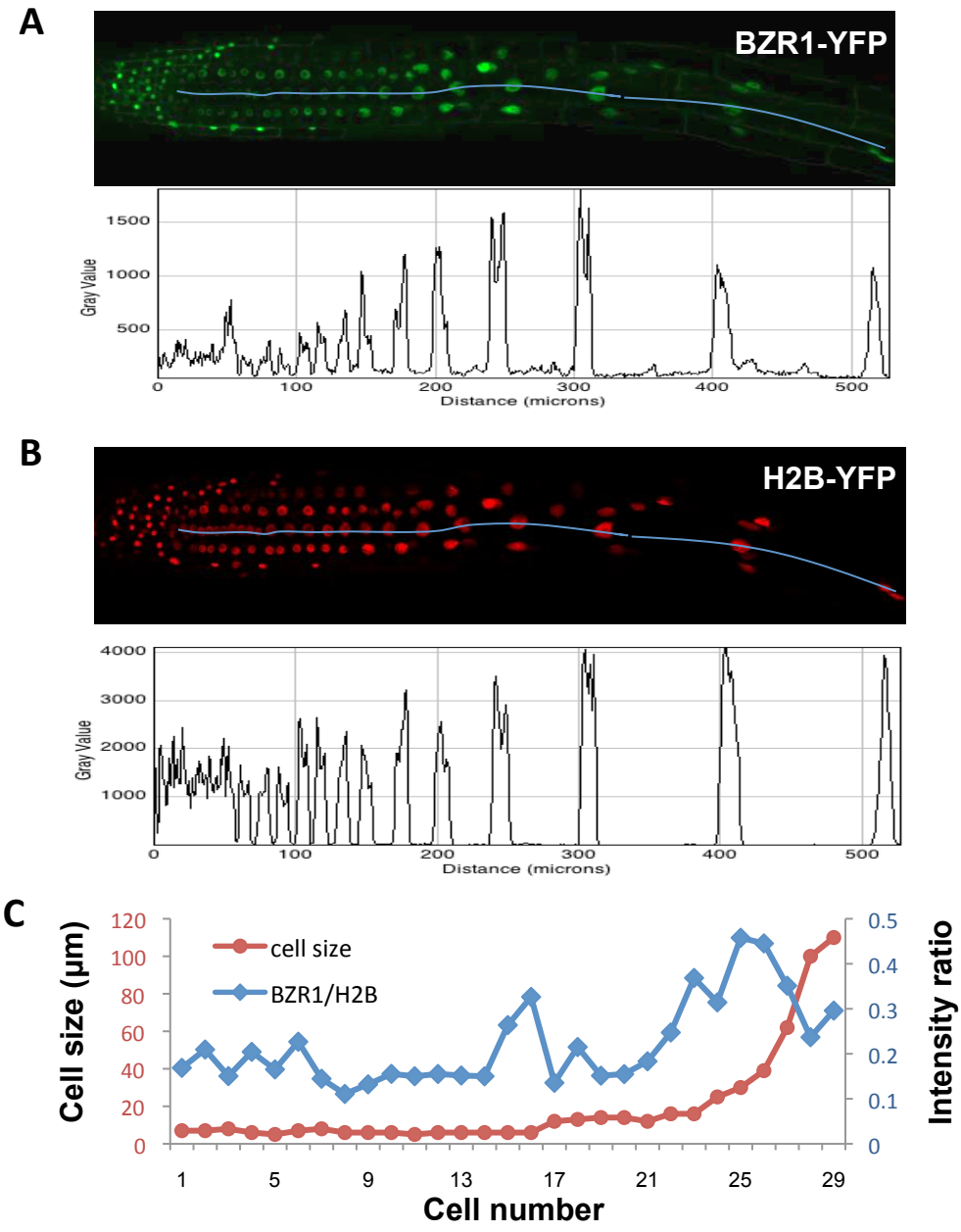

Figure S2. Nuclear BZR1 is patterned in root tip.
Confocal images of BZR1-YFP (A) and H2B-RFP (B) expressed in the same root. The YFP and RFP signal intensities were measured along the blue line and plotted in the graph below the images, using the Fiji software. (C) Quantitation of cell size and the ratio of BZR1-YFP to H2B-RFP signal intensities in the nuclei of the epidermal cells marked in panel A and B. Cells #15 and 16 are likely to have just finished division. See also Figure 2.

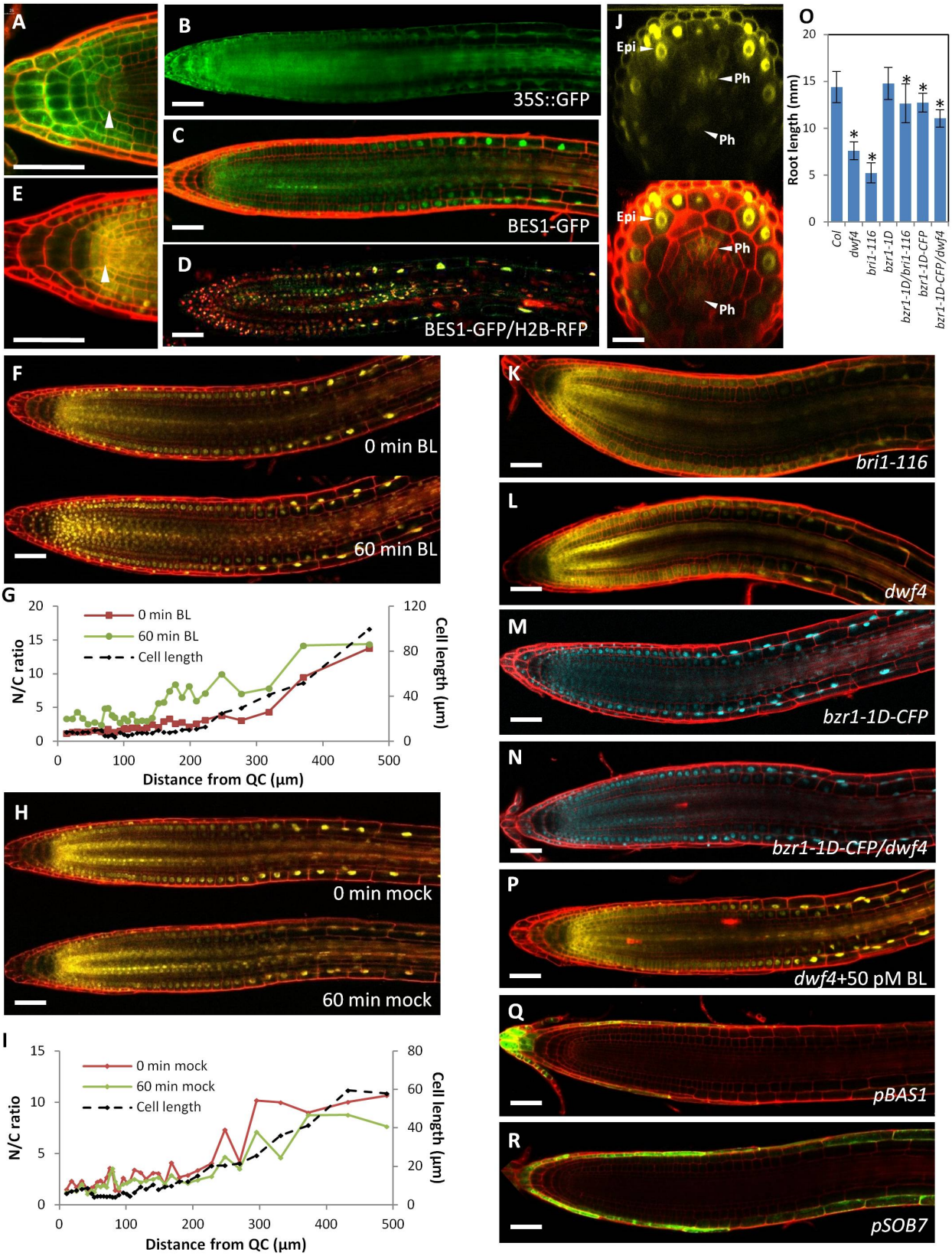

Figure S3. Spatial patterning of BR signaling and BR catabolism in roots.

Figure S3. Spatial patterning of BR signaling and BR catabolism in roots.
(A-B) Confocal images of root tips of *pBZR1:GFP* (A) and *35S:GFP* (B) transgenic plants. (C) *pBES1:BES1-GFP* root tip without treatment. (D) Overlay of confocal images of BES1-GFP (green) and H2B-RFP (red) expressed in the same root of a transgenic plant grown on regular medium. (E) Confocal image of a *pBZR1:BZR1-YFP* root tip. (F-I) Confocal images and quantification of nuclear to cytoplasmic (N/C) ratio and cell length in the epidermis along the root axis of *pBZR1:BZR1-YFP* root tips before and after 60 min treatment of BL (F-G) or mock (H-I). (J) Transverse section confocal images of the *pBZR1:BZR1-YFP* line showing accumulation of BZR1-YFP in the epidermis (Epi) and phloem (Ph). YFP channel (top), merged with propidium iodide stain (bottom). (K-L) BZR1-YFP protein is accumulated in the cytoplasm in the *bri1-116* and *dwf4* root tips. *pBZR1:BZR1-YFP*/*bri1-116* (K) and *pBZR1:BZR1-YFP/dwf4* (L) seedlings grown on regular medium. (M-N) bzr1-1D-CFP accumulates in nuclei of all cell types independently of endogenous BR biosynthesis. The *pBZR1:bzr1-1D-CFP* lines in the wild-type (M) or *dwf4* background (N) were grown on regular medium. (O) Root length of 6-day-old wild type Col-0 and indicated mutants (n>30, mean ±SD); * $P < 0.001$, as determined by a Student's t test. (P) *pBZR1:BZR1-YFP*/ *dwf4* seedling grown on medium containing 50 pM BL. (Q-R) Expression of *pBAS1:GFP* (Q) and *pSOB7:GFP* (R) in the root tip region. Scale bars, 50 µm. See also Figure 2.

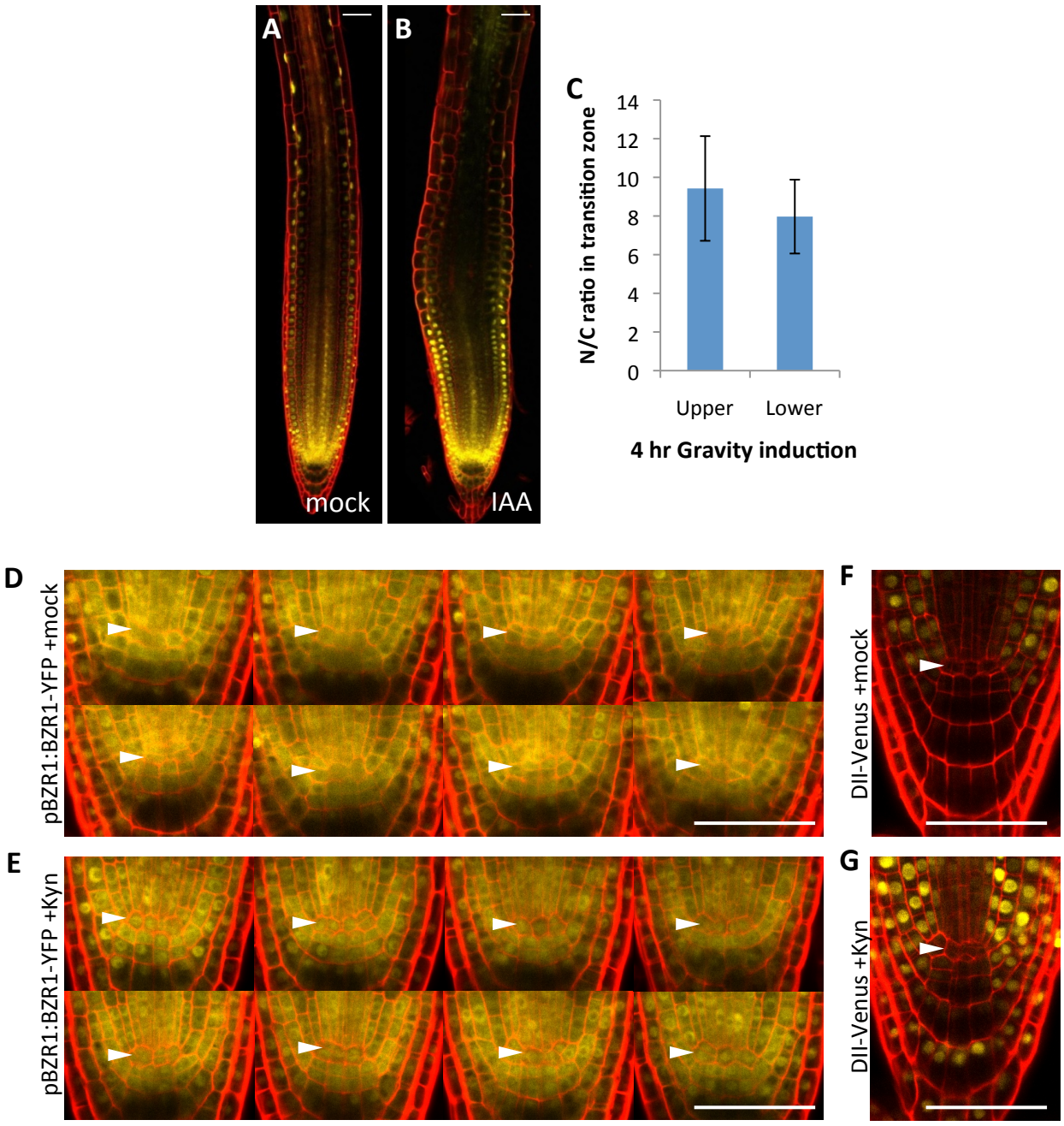

Figure S4. Effects of altered auxin distribution on BZR1 localization pattern.
(A-B) *pBZR1:BZR1-YFP* roots treated with mock (A) or 5 µM IAA (B) for 24 hr. (C) N/C ratios of BZR1-YFP in the transition zone (epidermis) of the upper and lower sides of *pBZR1:BZR1-YFP* roots after 4 hr gravity induction (n = 4 roots, mean ±SD). (D-E) Stem cell niche regions of *pBZR1:BZR1-YFP* roots treated with mock (D) or 25 µM L-Kynurenine (Kyn) (E) for 24 hr, n = 8. (F-G) Root tips of the *DII-Venus* auxin reporter treated with mock (F) or 25 µM Kyn (G) for 24 hr. Arrowheads indicate QC cell layer. Scale bars, 50 µm. See also Figure 4.

A

No. of BR regulated genes	Up	Down	Complex
BR treatment	1036 (40%)	722 (44%)	-
BR mutation	2519 (31%)	2142 (36%)	147
Total	2966	2345	134

*Percentage of BZR1 targets in parentheses

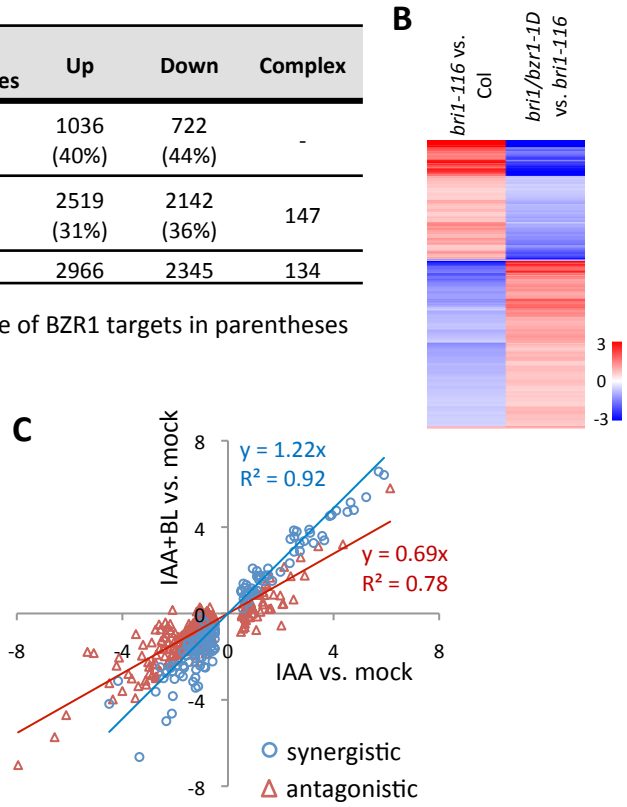

Figure S5. BR and auxin regulate overlapping transcriptomes.
(A) Table summarizing the number of genes induced (Up) or repressed (Down) by BR treatment (Col+BL vs. Col; *dwf4*+BL vs. *dwf4*) or BR mutation (Col vs. *dwf4*; Col vs. *bri1-116*; *bri1-116/bzr1-1D* vs. *bri1-116*) and the union of both sets (Total). 'Complex' indicates the number of genes respond to BR treatment or mutation in opposite manner. Percentages of BZR1 target genes are in parentheses. (B) Hierarchical cluster analysis of the genes affected by both *bri1-116* and *bzr1-1D*. The numerical values for the blue-to-red gradient bar represent $\log_2$ fold change relative to the control sample. (C) Scatter plot showing $\log_2$ fold change values of Col+IAA vs. Col and Col+IAA+BL vs. Col for genes affected by both IAA and BL single treatments in wild-type. See also Figure 5.

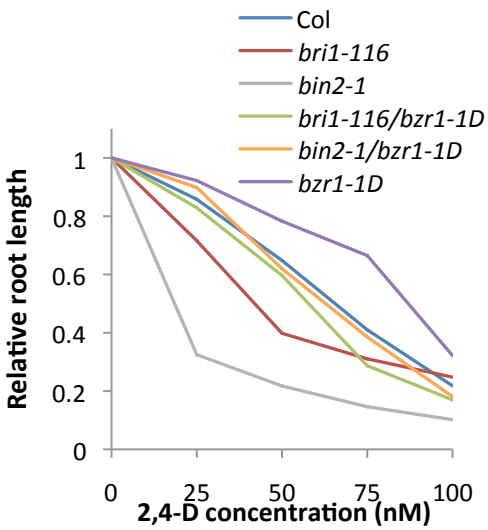

Figure S6. *bzr1-1D* suppresses the auxin hypersensitivity in root growth of BR-signaling mutants.

Relative root length of 6-day-old seedlings of indicated genotype grown on vertical media supplemented with various concentrations of 2,4-D. (n>30, mean ±SD). See also Figure 7.

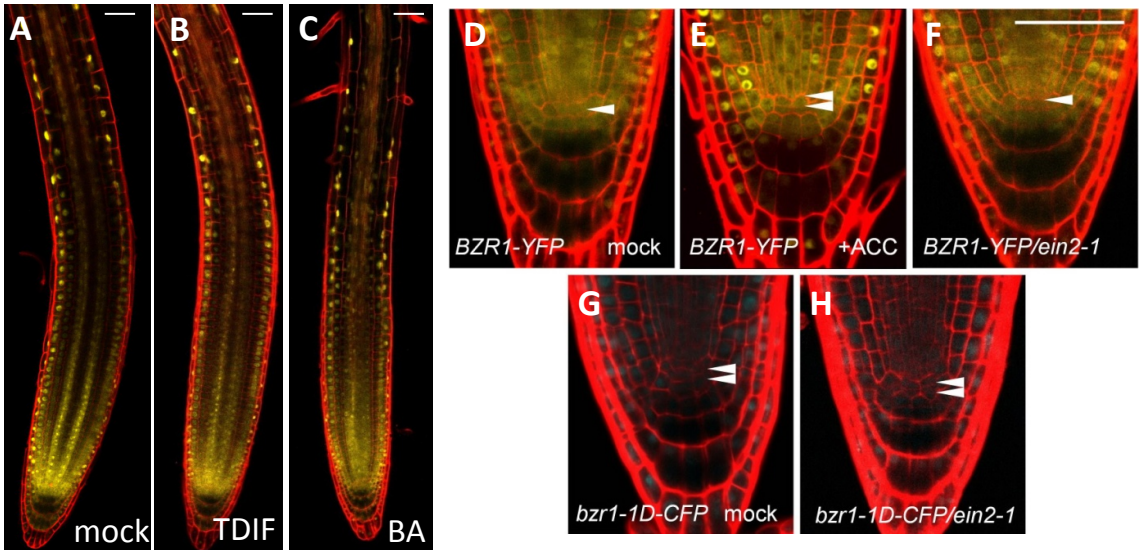

Figure S7. Patterning of BZR1 is independent of other signals and BZR1 regulates QC renewal independently of ethylene signaling.

pBZR1:BZR1-YFP roots treated with mock (A), 10 µM Tracheary Element Differentiation Inhibitory Factor (TDIF) (B), or 5 µM 6-benzylaminopurine (BA) (C) or for 24 hr. (D-E) Treatment of ethylene biosynthetic precursor ACC promotes QC division without promoting BZR1 nuclear accumulation in the QC. *pBZR1:BZR1-YFP* transgenic lines treated with mock (D) and 50 µM ACC (E) for 24 hr. (F) The *ein2-1* mutation does not alter BZR1 pattern in the root tip. The *pBZR1:BZR1-YFP* line in *ein2-1* background was grown on regular medium.

(G-H) The *ein2-1* mutant expressing *bzr1-1D-CFP* exhibits two layers of QC cells, like *bzr1-1D-CFP. pBZR1:bzr1-1D-CFP* in wild-type (G) or *ein2-1* background (H). Arrowheads indicate QC cell layer. Scale bars, 50 µm.

Supplemental Tables

Table S1. RNA-Seq data of BR- and auxin-responsive genes in roots showing average expression ratios and the *P*-values between indicated pair-wise comparisons.

Table S2. Comparison of genes up- or down-regulated by BR or auxin, identified by RNA-Seq in roots (Table S1), to the BZR1 ChIP-chip and ChIP-Seq data [S1, S2], and the RootMap spatial gene expression data [S3]. QC, quiescent center; MZ, meristem zone; TEZ, transition-elongation zone; LEZ, late elongation zone; DZ, differentiation zone.

Table S3. BR inhibits and auxin promotes ribosome biogenesis in meristem. Table includes genes related to ribosome biogenesis or rRNA processing among the meristem-enriched genes that are repressed by BR and induced by auxin. * indicates BZR1 target genes.

Gene_ID	Gene Name or Description
AT2G47990	SLOW WALKER1 (SWA1)
AT1G48920	NUCLEOLIN LIKE 1 (NUC-L1)
AT5G55920*	OLIGOCELLULA 2 (OLI2)
AT5G16750*	TORMOZEMBRYO DEFECTIVE (TOZ)
AT4G25630*	FIBRILLARIN 2 (FIB2)
AT3G55510*	REBELOTE (RBL)
AT5G61770*	PETER PAN-like protein (PPAN)
AT4G05410	YAOZHE (YAO)
AT3G60360	Embryo sac development arrest 14 (EDA14)
AT3G56990	Embryo sac development arrest 7 (EDA7)
AT1G31660	AtENP1/Putative bystin/protein co-factors of ribosome biogenesis
AT3G21540	Transducin/WD40 repeat-like superfamily protein
AT5G11240	Transducin/WD40 repeat-like superfamily protein
AT4G04940	Transducin/WD40 repeat-like superfamily protein
AT5G14050	Transducin/WD40 repeat-like superfamily protein
AT5G15550	Transducin/WD40 repeat-like superfamily protein
AT5G60990	DEA(D/H)-box RNA helicase family protein
AT5G65900	DEA(D/H)-box RNA helicase family protein
AT1G51380	DEA(D/H)-box RNA helicase family protein
AT5G54910	DEA(D/H)-box RNA helicase family protein
AT3G09720*	RNA Helicase 57 (RH57)
AT2G28600	RNA helicase/Yeast Dbp3p homolog/pre-rRNA processing/P-loop containing nucleoside triphosphate hydrolases superfamily protein
AT2G32220	Ribosomal protein L27e family
AT1G06380	Ribosomal protein L1p/L10e family
AT3G58660	Ribosomal protein L1p/L10e family

Gene_ID	Gene Name or Description
AT1G80750	Ribosomal protein L30/L7 family
AT5G39850	Ribosomal protein S4
AT3G57490	Ribosomal protein S5 family protein
AT5G59240	Ribosomal protein S8e family protein
AT1G03360	Ribosomal RNA processing 4 (RRP4)
AT5G40530	Ribosomal RNA-processing protein 8/S-adenosyl-L-methionine-dependent methyltransferases superfamily protein
AT1G52930	Ribosomal RNA processing Brix domain protein
AT1G60620	RNA polymerase I subunit 43 (RPAC43)
AT1G75670	DNA-dependent RNA polymerase I subunit RPA43
AT3G22660	rRNA processing protein-related
AT4G10620	BPG2-like/P-loop containing nucleoside triphosphate hydrolases superfamily protein
AT4G34910	P-loop containing nucleoside triphosphate hydrolases superfamily protein
AT2G40430	Gltscr2-homolog/nucleolar protein
AT1G79150*	Nucleolar complex-associated protein 3
AT1G63810	Nucleolar RNA-associated protein/U3 snoRNA-associated protein complex/Nrap protein
AT4G25730	FtsJ-like methyltransferase family protein
AT1G15420	Small-subunit processome, Utp12
AT3G19440	Pseudouridine synthase family protein
AT1G15440	Periodic tryptophan protein 2 (PWP2)
AT3G07750*	3'-5'-exoribonuclease family protein
AT5G66540	unknown protein

Table S4. Auxin regulates expression of genes involved in BR biosynthesis, BR catabolism and BR signaling pathway.

Auxin-responsive genes (Table S1, S2) with known function in BR biosynthesis, catabolism, and signaling pathway.

* Expression fold change from Col+IAA (5 µM, 4 hr) vs. Col comparison. Red = auxin-induced genes; blue = auxin-repressed genes.

	Gene name	Gene ID	BZR1target	BR	Auxin* (fold change, p<0.01)	QC	Zone
BR biosynthesis	DWF4	AT3G50660	yes	down	2.60	-	-
	CPD	AT5G05690	yes	down	0.64	-	-
	BR6OX1	AT5G38970	yes	up	0.26	-	TEZ
	ROT3/CYP90C1	AT4G36380	yes	no	0.62	-	TEZ
	CYP90D1	AT3G13730	yes	down	0.62	-	-
BR catabolism	BAS1	AT2G26710	yes	up	2.14	-	-
	SOB7/SHK1	AT1G17060	yes	up	4.57	-	TEZ
	BEN1	AT2G45400	no	up	3.73	-	TEZ
BR signaling	BRL1	AT1G55610	yes	down	4.11	QC	-
	BRL2	AT2G01950	no	up	0.55	-	-
	BRL3	AT3G13380	yes	down	6.74	-	-
	BKI1	AT5G42750	no	no	1.83	-	-

Table S5. BR pathway regulates expression of genes involved in auxin homeostasis and signaling pathway.

BR-regulated or BZR1 target genes with known function in auxin homeostasis and signaling pathway. Underlined = BZR1 target; red = BR-induced; blue = BR-repressed; black = non-BR-responsive; * = complex BR regulation.

AUX/IAA	ARF	Biosynthesis	Conjugation	Transport
IAA1	ARF2 (-)	TAR2	GH3.1	PIN1
IAA2	ARF9 (-)	TAA1	GH3.2	PIN3
IAA3	ARF18 (-)	YUC3	GH3.3	PIN5
IAA11	ARF19 (+)	YUC5	GH3.5	PIN2
IAA12	ARF4 (-)	YUC9	GH3.6	PIN4
IAA16	ARF10 (-)	YUC2	GH3.17	PIN6
IAA17	ARF11 (-)	YUC6*	GH3.18	PIN7
IAA18	ARF16 (-)	YUC8*	GH3.8	ENP
IAA19	ARF5 (+)	YUC4	GH3.14	PID2
IAA29	ARF8 (+)	TSA1	GH3.15	PID*
IAA10	ARF6 (+)	TSB1	GH3.10	PBP1*
IAA13	ARF17 (-)	TRP1	GH3.11	ABCB1
IAA14		CYP79B2		ABCB4
IAA33	**Receptor**	CYP79B3		ABCB19
IAA26	TIR1	ASA1		AUX1
IAA20	AFB2	ASB1		LAX1
IAA27		SUR1		LAX2
IAA30		NIT1		LAX3
		NIT2		WAG1
		NIT3		WAG2
				WAT1

Supplemental Movie

Movie S1: A three-dimensional view of BZR1-YFP (green) and H2B-RFP (red) expressed from the *35S* promoter in a root of transgenic plant grown on regular medium. Serial optical sections (Z-stack, 2 µm each) were processed using Fiji software package to render 3-D view. See also Figure 2B.

Supplemental Experimental Procedures

Plant growth and root imaging

All wild-type, various mutants and transgenic lines are in the *Arabidopsis thaliana* Columbia (Col-0) background. These include *dwf4* (Salk_020761), *bri1-116* [S4], *bin2-1* [S5], *bzr1-1D* [S6], *bri1-116/bzr1-1D* [S7], *bin2-1/bzr1-1D, pBZR1:bzr1-1D-CFP* [S8], *bas1-2/sob7-1* [S9], *ein2-1* [S10], *pBZR1:BZR1-YFP* [S11], *pBRAVO:GFP* [S12]; *pPLT1:PLT1-YFP* and *pPLT2:PLT2-YFP* [S13], and *35S:H2B-RFP* [S14]. Seeds were surface sterilized for 15 min with 70% ethanol/0.05% Triton X-100 solution and plated on half-strength MS media pH 5.7, containing 1% sucrose and 0.8% Phytoblend agar. Seedlings were grown vertically on regular media, supplemented with hormones or mock under constant light. An auxin analog, 2,4-D, was used in auxin root inhibition assays because the natural auxin IAA is significantly degraded over long-term treatment [S15].

Root lengths were measured from images using ImageJ. For live-imaging analysis, seedlings were grown on regular media for 5 days and then transferred to new media supplemented with hormones or mock, and imaged every 15 min for 3 days using a custom macroscopic imaging system as previously described [S16]. Sequential images were aligned and stacked using ImageJ. Quantification of root growth was performed using a macro in ImageJ as previously described [S17].

Confocal microscopy and quantification of fluorescence signal

Laser scanning confocal microscopy was performed by using a Leica SP5 system after propidium iodide staining. At least 5 roots were analyzed for each treatment in each experiment and each experiment was repeated independently at least 3 times. The same laser settings were

used within the same experiment. To determine N/C ratios of BZR1-YFP, BES1-GFP and bzr1-1D-CFP, the transgenic lines were crossed with plants expressing a nuclear marker *35S:H2B-RFP*, and serial optical sections were obtained from roots of F1 seedlings. Mean fluorescence intensities of nuclear and cytoplasmic areas of each epidermal cell along the root axis and QC cells were measured from the optical section that passed through the center of the nucleus of each cell using Fiji (http://fiji.sc/wiki/index.php/Fiji). For comparison of nuclear and cytoplasmic BZR1-YFP signals before and after BL treatment, mean fluorescence intensities were measured from the same corresponding cells. Quantification of BZR1-YFP in QC cells of the *bas1/sob7* mutants were performed with confocal images that passed through the center of QC's nuclei. For gravity-induction experiments, vertically grown BZR1-YFP seedlings were mounted on slides and maintained in horizontal position to stimulate gravitropism for 4 hr. The root epidermis was then imaged from both upper and lower sides of the roots. Nuclear and cytoplasmic BZR1-YFP signals were measured from five epidermal cells in the transition zone from each side of the roots. The average N/C ratio was then calculated from measurements of four roots.

Plasmid construction and transformation

To generate the *pWOX5:bzr1-1D-YFP, pSCR:bzr1-1D-YFP,* and *pWER:bzr1-1D-YFP* constructs, the coding sequence of *bzr1-1D-YFP* was cloned from cDNA into the GATEWAY entry vector pENTRY/SD/D-TOPO (Invitrogen). The *WOX5* promoter region was cloned from genomic DNA into pDONR-P4P1R.Constructs with 2.5 kb 5' fragment and 1.1 kb 3' fragment of *WER*, as well as 2 kb 5'fragment of *SCR* are gift from J. Dinneny. The multisite gateway recombination was used to introduce the promoter fragment, the coding sequence and 3' fragment into a dpGreen-based binary vector with mCherry selection marker for plant selection [S16]. To generate the *pBES1:BES1-GFP* construct, *BES1* promoter and coding sequence was

cloned into the GATEWAY entry vector and recombined into the destination vector pGWB4. To generate the *BZR1, BAS1,* and *SOB7* promoter reporter constructs, the 1.0 kb, 2.9 kb, and 2.3 kb upstream regions of *BZR1*, *BAS1*, and *SOB7*, respectively, were amplified from Col-0 genomic DNA. The promoter fragments and the GFP reporter were then assembled into pGoldenGate-SE7 destination vector as previously described [S18]. The constructs were transformed into *Arabidopsis* via *Agrobacterium tumefaciens* GV3101. All primers used for cloning are listed in the following table.

Primers used for cloning in this study

Name	**Sequence**
WOX5pro-F	GGGGACAACTTTGTATAGAAAAGTTGCGAGAACCTCGGGGATGAAGAC
WOX5pro-R	GGGGACTGCTTTTTTGTACAAACTTGCGTTCAGATGTAAAGTCCTCAACTGTTT
BZR1pro-F	CACCGGTCTCAAGTAGCCTAATTCATCGAACCCTCT
BZR1pro-R	TTTGGTCTCATCATCGGGAAAACCAACAACCAA
BAS1pro-F	CACCGGTCTCAAGTAGTATATCATGTATACTTAT
BAS1pro -R	TTTGGTCTCATCATTTGAGTGCCGGAGAAAGA
SOB7pro -F	CACCGGTCTCAAGTAGACTGCAAATCGCCGACGT
SOB7pro -R	TTTGGTCTCATCATCTTGATCTAGCTATGAAGA
BES1pro -F	CACCAAGTTGTCACTAAGATCGG
BES1-R	ACTATGAGCTTTACCATTTCCAAG

Total RNA extraction and quantitative RT-PCR analysis

Seedlings were grown vertically on regular media in constant light for 7 days and treated with 100 nM BL, 5 μM IAA, 100 nM BL+5 μM IAA or ethanol (mock) solution for 4 hr. Roots were sectioned in the middle and the root tip half was harvested for total RNA extraction using the Spectrum Plant Total RNA kit (Sigma). For quantitative RT-PCR (qRT-PCR), the total RNA was used to prepare the first-strand cDNA using RevertAid reverse transcriptase (Fermentas).

Quantitative RT-PCR was performed on LightCycler 480 (Roche) using a SYBR Green reagent (Bioline). Three biological replicates were used in the analysis. All primers used in qRT-PCR analysis are listed in the following table.

Primers used in qRT-PCR analysis

Name	Sequence of qRT-PCR primers
EXPA8-qF	TCCTCCTCTTCAGCATTTCGACCT
EXPA8-qR	CTTGCCACGACTGTGTTTTTGAGC
ACS5-qF	GCGATGCTTTCCTTTTGCCTACTC
ACS5-qR	TTTCTGGGCTTGTTGGTAAGCTTGT
ACS11-qF	GCTGAAAACCAGCTTTCTTTTG
ACS11-qR	TTTGTTCTCTCTGATTTTCCC
DWF4-qF	CATAAAGCTCTTCAGTCACGA
DWF4-qR	CGTCTGTTCTTTGTTTCCTAA
IAA19-qF	GGTGACAACTGCGAATACGTTACCA
IAA19-qR	CCCGGTAGCATCCGATCTTTTCA

RNA-Seq

The mRNA sequencing libraries were constructed with barcodes using the TruSeq RNA Sample Preparation kit (Illumina) according to manufacturer's instructions. The libraries were pooled and sequenced by Illumina HiSeq2000 with two biological replicates for each condition. The 36-bp sequence reads of *dwf4, dwf4*+BL and wild-type and the 101-bp sequence reads of Col, Col+BL, Col+IAA, Col+IAA+BL, *bri1-116, bri1-116/bzr1-1D* were aligned to the *Arabidopsis* genome, TAIR10, using TopHat software [S19]. Read counts for each gene were quantified using HTSeq-count with union mode. Differential expression was determined using DESeq [S20] with fold change > 1.4 (equivalent to $\log_2$ fold change > 0.5), $P < 0.01$. Enrichment analysis was performed using the DAVID Functional Annotation tool [S21] for both GO

categories and InterPro protein families. Heatmaps of *P*-values were generated by matrix2png [S22]. Expression data were clustered or sorted and visualized with the TIGR MeV program [S23].

Supplemental References

S1. Oh, E., Zhu, J.-Y., Bai, M.-Y., Arenhart, R. a, Sun, Y., and Wang, Z.-Y. (2014). Cell elongation is regulated through a central circuit of interacting transcription factors in the Arabidopsis hypocotyl. Elife, e03031.

S2. Sun, Y., Fan, X.-Y., Cao, D.-M., Tang, W., He, K., Zhu, J.-Y., He, J.-X., Bai, M.-Y., Zhu, S., Oh, E., et al. (2010). Integration of brassinosteroid signal transduction with the transcription network for plant growth regulation in Arabidopsis. Dev. Cell *19*, 765–77.

S3. Brady, S. M., Orlando, D. a, Lee, J.-Y., Wang, J. Y., Koch, J., Dinneny, J. R., Mace, D., Ohler, U., and Benfey, P. N. (2007). A high-resolution root spatiotemporal map reveals dominant expression patterns. Science *318*, 801–6.

S4. Friedrichsen, D. M., Joazeiro, C. a, Li, J., Hunter, T., and Chory, J. (2000). Brassinosteroid-insensitive-1 is a ubiquitously expressed leucine-rich repeat receptor serine/threonine kinase. Plant Physiol. *123*, 1247–56.

S5. Li, J., Nam, K. H., Vafeados, D., and Chory, J. (2001). BIN2, a new brassinosteroid-insensitive locus in Arabidopsis. Plant Physiol. *127*, 14–22.

S6. Wang, Z. Y., Nakano, T., Gendron, J., He, J., Chen, M., Vafeados, D., Yang, Y., Fujioka, S., Yoshida, S., Asami, T., et al. (2002). Nuclear-localized BZR1 mediates brassinosteroid-induced growth and feedback suppression of brassinosteroid biosynthesis. Dev. Cell *2*, 505–13.

S7. Gendron, J. M., Haque, A., Gendron, N., Chang, T., Asami, T., and Wang, Z.-Y. (2008). Chemical genetic dissection of brassinosteroid-ethylene interaction. Mol. Plant *1*, 368–79.

S8. He, J.-X., Gendron, J. M., Yang, Y., Li, J., and Wang, Z.-Y. (2002). The GSK3-like kinase BIN2 phosphorylates and destabilizes BZR1, a positive regulator of the brassinosteroid signaling pathway in Arabidopsis. Proc. Natl. Acad. Sci. U. S. A. *99*, 10185–90.

S9. Turk, E. M., Fujioka, S., Seto, H., Shimada, Y., Takatsuto, S., Yoshida, S., Wang, H., Torres, Q. I., Ward, J. M., Murthy, G., et al. (2005). BAS1 and SOB7 act redundantly to modulate Arabidopsis photomorphogenesis via unique brassinosteroid inactivation mechanisms. Plant J. *42*, 23–34.

S10. Guzman, P., and Ecker, J. (1990). Exploiting the triple response of Arabidopsis to identify ethylene-related mutants. Plant Cell *2*, 513–523.

S11. Gendron, J. M., Liu, J.-S., Fan, M., Bai, M.-Y., Wenkel, S., Springer, P. S., Barton, M. K., and Wang, Z.-Y. (2012). Brassinosteroids regulate organ boundary formation in the shoot apical meristem of Arabidopsis. Proc. Natl. Acad. Sci. U. S. A. *109*, 21152–21157.

S12. Vilarrasa-Blasi, J., González-García, M.-P., Frigola, D., Fàbregas, N., Alexiou, K. G., López-Bigas, N., Rivas, S., Jauneau, A., Lohmann, J. U., Benfey, P. N., et al. (2014). Regulation of Plant Stem Cell Quiescence by a Brassinosteroid Signaling Module. Dev. Cell, 1–12.

S13. Galinha, C., Hofhuis, H., Luijten, M., Willemsen, V., Blilou, I., Heidstra, R., and Scheres, B. (2007). PLETHORA proteins as dose-dependent master regulators of Arabidopsis root development. Nature *449*, 1053–7.

S14. Federici, F., Dupuy, L., Laplaze, L., Heisler, M., and Haseloff, J. (2012). Integrated genetic and computation methods for in planta cytometry. Nat. Methods *9*, 483–5.

S15. Dunlap, J. R., Kresovich, S., and McGee, R. E. (1986). The effect of salt concentration on auxin stability in culture media. Plant Physiol. *81*, 934–6.

S16. Duan, L., Dietrich, D., Ng, C. H., Chan, P. M. Y., Bhalerao, R., Bennett, M. J., and Dinneny, J. R. (2013). Endodermal ABA signaling promotes lateral root quiescence during salt stress in Arabidopsis seedlings. Plant Cell *25*, 324–41.

S17. Geng, Y., Wu, R., Wee, C. W., Xie, F., Wei, X., Chan, P. M. Y., Tham, C., Duan, L., and Dinneny, J. R. (2013). A Spatio-Temporal Understanding of Growth Regulation during the Salt Stress Response in Arabidopsis. Plant Cell *25*, 2132–54.

S18. Emami, S., Yee, M.-C., and Dinneny, J. R. (2013). A robust family of Golden Gate Agrobacterium vectors for plant synthetic biology. Front. Plant Sci. *4*, 339.

S19. Trapnell, C., Pachter, L., and Salzberg, S. L. (2009). TopHat: discovering splice junctions with RNA-Seq. Bioinformatics *25*, 1105–11.

S20. Anders, S., and Huber, W. (2010). Differential expression analysis for sequence count data. Genome Biol. *11*, R106.

S21. Huang, D. W., Sherman, B. T., Tan, Q., Collins, J. R., Alvord, W. G., Roayaei, J., Stephens, R., Baseler, M. W., Lane, H. C., and Lempicki, R. A. (2007). The DAVID Gene Functional Classification Tool: a novel biological module-centric algorithm to functionally analyze large gene lists. Genome Biol. *8*, R183.

S22. Pavlidis, P., and Noble, W. (2003). Matrix2png: a utility for visualizing matrix data. Bioinformatics *19*, 295–296.

S23. Saeed, A., Sharov, V., White, J., and Li, J. (2003). TM4: a free, open-source system for microarray data management and analysis. Biotechniques *34*, 374–378.